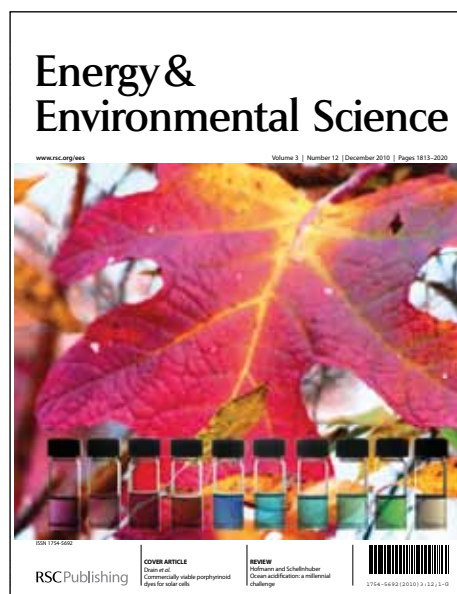


Energy & Environmental Science

Accepted Manuscript



This is an *Accepted Manuscript*, which has been through the RSC Publishing peer review process and has been accepted for publication.

Accepted Manuscripts are published online shortly after acceptance, which is prior to technical editing, formatting and proof reading. This free service from RSC Publishing allows authors to make their results available to the community, in citable form, before publication of the edited article. This *Accepted Manuscript* will be replaced by the edited and formatted *Advance Article* as soon as this is available.

To cite this manuscript please use its permanent Digital Object Identifier (DOI®), which is identical for all formats of publication.

More information about *Accepted Manuscripts* can be found in the [Information for Authors](#).

Please note that technical editing may introduce minor changes to the text and/or graphics contained in the manuscript submitted by the author(s) which may alter content, and that the standard [Terms & Conditions](#) and the [ethical guidelines](#) that apply to the journal are still applicable. In no event shall the RSC be held responsible for any errors or omissions in these *Accepted Manuscript* manuscripts or any consequences arising from the use of any information contained in them.

Cite this: DOI: 10.1039/c0xx00000x

ARTICLE TYPE

www.rsc.org/xxxxxx

Air-Stable, High-Conduction Solid Electrolytes of Arsenic-Substituted Li_4SnS_4 Gayatri Sahu,¹ Zhan Lin,² Juchuan Li,² Zengcai Liu,¹ Nancy Dudney,² and Chengdu Liang^{1*}

Received (in XXX, XXX) Xth XXXXXXXXXX 20XX, Accepted Xth XXXXXXXXXX 20XX

DOI: 10.1039/b000000x

Lithium-ion-conducting solid electrolytes show promise for enabling high-energy secondary battery chemistries and solving safety issues associated with conventional lithium batteries. Achieving the combination of high ionic conductivity and outstanding chemical stability in solid electrolytes is a grand challenge for the synthesis of solid electrolytes. Herein we report the design of aliovalent substitution of Li_4SnS_4 to achieve high conduction and excellent air stability based on the hard and soft acids and bases theory. The composition of $\text{Li}_{3.833}\text{Sn}_{0.833}\text{As}_{0.166}\text{S}_4$ has a high ionic conductivity of 1.39 mS/cm^{-1} at 25°C . Considering the high Li^+ transference number, this phase conducts Li^+ as well as carbonate-based liquid electrolytes. This research also addresses the compatibility of the sulfide-based solid electrolytes through chemical passivation.

Introduction

The future of sustainable energy lies in the harvesting and delivery of renewable energy supplies that are intermittent. Energy storage is critical to enable a stable supply of energy from intermittent energy sources. Although lithium-ion (Li-ion) batteries are widely used in portable electronics, their limited energy density and relatively high cost prohibit their application in large-scale energy storage for wind and solar energy, or as the power supplies for fully electric vehicles with a desirable driving range of 300–500 miles per charge. To meet these needs, Li-sulfur (Li-S) batteries have the potential to improve the energy density of Li-ion batteries by a factor of 4 while significantly reducing battery material costs. High-energy Li-S batteries rely on conversion chemistry, rather than the insertion chemistry that is the signature of Li-ion batteries. Their practical application, though, is currently limited by the formation of polysulfides in the liquid electrolytes.^{1,2} These polysulfide shuttles diminish the performance of Li anodes, leading to electrode degradation and decreased coulombic efficiency. In addition, the notorious safety issue associated with cycling metallic Li in flammable liquid electrolytes prevent the deployment of Li-S batteries.

Recently, we found that Li-S batteries can be cycled very well in an all-solid-state configuration.^{3,4} All-solid-state Li secondary batteries employing inorganic solid electrolytes have attracted much attention because of their safety, reliability, resistance to leakage, compatibility with high-capacity active materials, and superior mechanical and thermal stability.^{5,6} There are quite promising reports in the search for new solid electrolytes, such as $\beta\text{-Li}_3\text{PS}_4$ ⁷⁻⁹ perovskites,¹⁰ $\text{Li}_2\text{S-P}_2\text{S}_5$ glass-based sulfide solid electrolytes,^{11,12} and glass ceramic $\text{Li}_7\text{P}_3\text{S}_{11}$.¹³ A novel Li superionic conductor, $\text{Li}_{10}\text{GeP}_2\text{S}_{12}$ (LGPS), a member of the thio-LISICON family,^{14,15} has reached an unprecedented high ionic

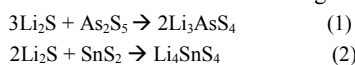
conductivity of $1.2 \times 10^{-2} \text{ S cm}^{-1}$.¹⁶ In general, sulfides have higher ionic conductivity than oxides but lower air and moisture stability than oxides.¹⁷ The hypersensitivity of the thio-LISICONS to air and moisture requires sophisticated and tedious treatment under a dry inert gas atmosphere, which increases their processing cost. The stability of the sulfides follows the rules of the hard and soft acids and bases (HSAB) theory. Soft acids are larger, have a more diffused distribution of electrons, and are more easily polarized compared with hard acids, which are small, compact, and non-polarizable. According to the HSAB theory, hard acids react preferentially with hard bases, and soft acids are more prone to react with soft bases. Based on the HSAB theory, thiophosphate-based superionic conductors are chemically unstable against oxygen because oxygen is a hard base that reacts preferentially with the hard acid P to replace the soft base S.

We report herein a high-conduction sulfide-based solid electrolyte with superior air stability based on the HSAB theory. The soft acids Sn and As were selected as the center elements to form compounds with sulfur and therefore impart excellent chemical stability against oxygen, which is a considerably harder base than sulfur. Tetralithium *ortho*-sulfidostannate Li_4SnS_4 has a promising Li^+ ion conductivity of $7 \times 10^{-5} \text{ S cm}^{-1}$ at 20°C .¹⁸ It is interesting to note that anhydrous Li_4SnS_4 can be produced from its hydrated form through direct dehydration without hydrolysis and oxidation from air. The same excellent stability against water and oxygen is expected for Li_3AsS_4 because As is a soft acid. Replacing P with As provides an obvious advantageous stability against oxygen and water. The issues addressed in this work are twofold: (1) Can an aliovalent cation of As enhance the conductivity of Li_4SnS_4 ? (2) Does the As-substituted Li_4SnS_4 have the expected air and moisture stability?

Experimental

Synthesis of As-substituted Li_4SnS_4 [$\text{Li}_{4-x}\text{Sn}_{1-x}\text{As}_x\text{S}_4$ (where, $x = 0$ to 0.250)]

The as-received starting materials of Li_2S (Sigma-Aldrich, 99.9% purity), SnS_2 (vendor, 99.9% purity), and As_2S_5 (vendor, 99.9% purity) were used in the synthesis without further purification. All materials were weighed and mixed in required molar ratios of $\text{Li}_2\text{S}:\text{As}_2\text{S}_5:\text{SnS}_2$ in an argon-filled glove box. The mixtures were placed in an agate mortar and pestle and hand ground for 30 min. The molar ratios were determined maintaining a trend in the As-to-Sn ratio based on the following two reactions:



The powder mixture was then sealed in Pyrex glass tubes under house vacuum. The reaction was conducted at 450°C for 12 h and then slowly ramped down to 350°C in 12 h. The final product was slowly cooled down from 350°C to room temperature in 4 h.

Structural characterization

Powder x-ray diffraction (XRD) patterns were collected on an X'pert Pro powder diffractometer (PANalytical) with a copper $\text{K}\alpha$ line. Although the materials are not air-sensitive, to avoid possible interference from absorbed moisture, the XRD samples were covered by Kapton films to avoid moisture uptake.

Ionic conductivity measurements

All materials were cold-pressed into dense pellets under 300 Mpa for the measurement of ionic conductivity. Pellets (diameter 1.27 cm, thickness ~ 0.06 cm) were prepared by pressing the powder with carbon-coated aluminum foils (a free sample from Exopack) on both sides in an argon-filled glove box. The carbon-coated aluminum foils served as blocking electrodes. Electrochemical impedance spectroscopy (EIS) measurements were carried out using a specially designed air-tight cell. The ac impedance measurements were conducted in the frequency range of 1 MHz to 1 Hz with an amplitude of 5 mV using a frequency response analyzer (Solartron 1260). For the Arrhenius plot, temperature was ramped from 25 to 100°C and returned to 25°C in a temperature chamber (Maccor). The accuracy of the temperature was within $\pm 0.5^\circ\text{C}$. An EIS spectrum is presented in Fig. S1. The Nyquist plot shows a typical semicircle at higher frequency region that represents the bulk and grain boundary resistance of the electrolyte and a spike at lower frequency region that represents the diffusion due to blocking electrode, a characteristic feature expected for pure ionic conductors. The intercept of the spike at the axis of $Z'(\Omega)$ was employed to determine the total ionic conductivity.

Symmetric cell fabrication and Li cyclability measurements

Because of the chemical reaction of the solid electrolyte with metallic Li, the symmetric cell test was conducted on a passivated pellet. The passivation solution is a mixture of Li borohydride and Li iodide with a molar ratio of 3:1 in tetrahydrofuran (THF). The concentration is 5 wt. of solid content in THF. The composition of the 3:1 molar ratio LiBH_4/LiI is expected to be a high-conduction solid electrolyte that is compatible with metallic Li.¹⁹ The coating was applied by dipping the $\text{Li}_{3.833}\text{Sn}_{0.833}\text{As}_{0.166}\text{S}_4$ pellet into the composite solution and

vacuum drying at 170°C for 1 h. Two pieces of Li foil were attached to the coated pellet for a symmetric cell test. The symmetric cells were cycled on a battery test system (Maccor 4000) with a current density of 0.1 mAcm^{-2} at room temperature.

Electrochemical Characterization

The cyclic voltammogram (CV) was measured on a $3\text{LiBH}_4.\text{LiI}$ in THF coated $\text{Li}/\text{Li}_{3.833}\text{Sn}_{0.833}\text{As}_{0.166}\text{S}_4/\text{Pt}$ cell where Li and Pt serve as the reference and counter electrodes respectively. The potential was scanned from -0.5 to 5.0 V vs. Li/Li^+ at a scan rate of 1 mVs^{-1} between -0.5V and 5.0 V at room temperature by using a potentiostat (Bio-Logic VMP3).

Electronic Conductivity Measurements

The DC polarization measurement was conducted to determine the electronic conductivity of the solid electrolyte. Each side of a cold pressed pellet (diameter 1.27 cm, thickness ~ 0.06 cm) was coated with 100 nm Au (99.9999%) serving as the blocking electrodes. The pellet was sealed in a Swagelok cell in Ar filled glove box. Conductivity measurement was carried out using a potentiostat (Bio-Logic VMP3) with low-current probe where the lowest measurable current is smaller than 1 pA. The voltage was held at each step for 10 hours, and the stabilized current was recorded as an indication of the electronic conductivity. A Faraday cage was used during the measurement. The electronic conductivity and ionic transference number of $\text{Li}_{3.833}\text{Sn}_{0.833}\text{As}_{0.166}\text{S}_4$ were measured.

Results and discussion

Effect of As substitution on the ionic conductivity of Li_4SnS_4

The As substitution into Li_4SnS_4 gives a general formula of $\text{Li}_{4-x}\text{Sn}_{1-x}\text{As}_x\text{S}_4$ (where $x=0$ to 0.250). Li_4SnS_4 serves as the base material to form the matrix. Li_3AsS_4 is the minor component. The ionic conductivity of the samples for various molar ratios of As to Sn were studied as a function of the temperature. Figure 1a represents typical Arrhenius plots for the Li-ion conductivity in the range of 25 to 100°C. The activation energies E_a for the conduction were calculated using the equation

$$\sigma_T = \sigma_o \exp(-E_a/k\beta T), \quad (3)$$

where σ_T is the total electrical conductivity, σ_o is the pre-exponential parameter, T is absolute temperature, E_a is the activation energy, and k_β is the Boltzmann constant. Figure 1b presents the room-temperature ionic conductivity (left y-axis) and activation (right y-axis) energy versus composition. The pristine Li_4SnS_4 has an ionic conductivity of $7.1 \times 10^{-5} \text{ S cm}^{-1}$ at 25°C, which is consistent with the literature value.¹⁸ Low-concentration doping of As is actually causing a decrease in ionic conductivity. The composition of $\text{Li}_{3.875}\text{Sn}_{0.875}\text{As}_{0.125}\text{S}_4$ ($x=0.125$) has an ionic conductivity of $1.48 \times 10^{-5} \text{ Scm}^{-1}$. The ionic conductivity increases as the As substitution increases and reaches a maximum at $x=0.166$. The highest conductivity achieved is $1.39 \times 10^{-3} \text{ Scm}^{-1}$ at 25°C with the composition $\text{Li}_{3.833}\text{Sn}_{0.833}\text{As}_{0.166}\text{S}_4$. The electronic conductivity was measured through the DC polarization measurements, which gave a value of $1.5 \times 10^{-9} \text{ Scm}^{-1}$. The calculated Li^+ transference number is 0.9999, which is

considerably higher than liquid^{20, 21} and polymer²² electrolytes.

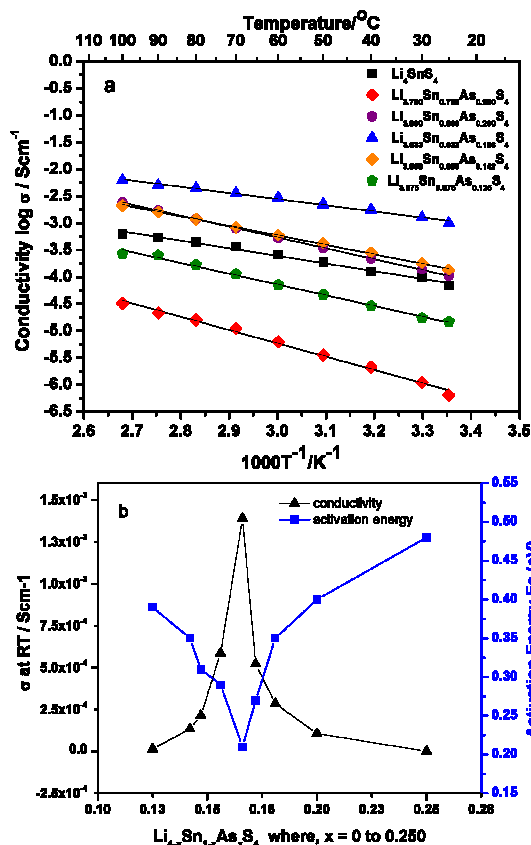


Fig. 1 (A) Arrhenius plot of ionic conductivity of Li_4SnS_4 and As-doped Li_4SnS_4 , i.e. $\text{Li}_{4-x}\text{Sn}_{1-x}\text{As}_x\text{S}_4$ (where $x=0$ to 0.250) with various molar ratios of As:Sn. The top x-axis is temperature and the bottom x-axis is $1000/T$. (B) Room-temperature ionic conductivity (left y-axis) and activation energies (right y-axis) as a function of composition.

Considering Li^+ as the only mobile species in the solid electrolyte, the conduction of Li^+ in this solid electrolyte is comparable to that of the currently used carbonate-based liquid electrolytes.

It is worth noting that the activation energy versus the concentration of As substitution displays as an inverted peak of the conductivity (Fig. 1b). The lowest activation energy was observed in the composition of $\text{Li}_{3.833}\text{Sn}_{0.833}\text{As}_{0.166}\text{S}_4$ that had the highest ionic conductivity. The activation energy was as low as 0.21 eV as compared to other well-known solid electrolytes.^{9, 16, 23, 24} A detailed comparison of activation energy of known electrolytes was provided in Table S1. Such a low activation energy ensures a flat conductivity curve in a broad temperature range. This characteristic favors a stable performance when the material is used in a broad temperature range. In other words, a battery with such a solid electrolyte will not have the sudden performance drop that is expected in liquid electrolytes when the temperatures rise beyond the liquidus temperature of the organic solvents.

As substitution forms solid solution phase

All XRD patterns (Fig. 2) show that the matrix of $\text{Li}_{4-x}\text{Sn}_{1-x}\text{As}_x\text{S}_4$ (where $x=0$ to 0.250) is Li_4SnS_4 (space group Pnma,

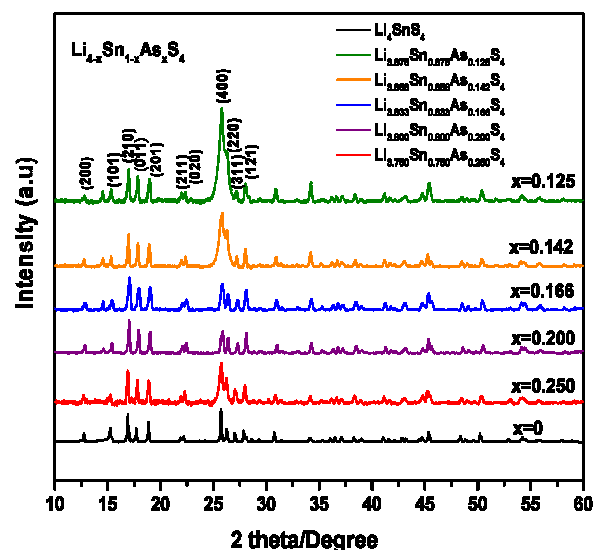


Fig. 2 Structural evaluation. XRD patterns of Li_4SnS_4 and As-substituted Li_4SnS_4 , i.e., $\text{Li}_{4-x}\text{Sn}_{1-x}\text{As}_x\text{S}_4$ (where $x=0$ to 0.250) with peaks indexed for orthorhombic crystal pattern.

$a=13.812(3)$ Å, $b=7.9624(16)$ Å, $c=6.3670(13)$ Å).¹⁸ A series of 25 peaks from 2θ of 10 to 35° are assigned as the following: 12.8° (200); 15.3° (101); 17.04° (210); 17.8° (011); 18.9° (201); 22.04° (211); 22.3° (020); 25.5° (400); 26.4° (220); 27.2° (311); and 28.1° (121).¹⁸ In the concentration range from $x=0$ to 0.25, no peak was identified as Li_3AsS_4 . This is a clear piece of evidence for the formation of solid solutions of Li_3AsS_4 in Li_4SnS_4 . Significant peak broadening was observed in all As-substituted samples. The ionic radius of As^{5+} is 60 pm, which is considerably smaller than the 83 pm radius of Sn^{4+} .²⁵ The peak broadening results from a disordering of the crystal structure due to the substitution of As atoms for the Sn atoms at the metal centers of the tetrahedron $[\text{SnS}_4]^{4+}$ units. The substitution creates interstitials or vacancies that are accounted from the enhanced ionic conductivity of the solid solutions. Three additional weak peaks appear at 2θ of 14.56° , 29.42° , and 35.27° . These peaks could originate from the As atoms of the solid solutions.

The recently discovered phases of $\text{Li}_{10}\text{GeP}_2\text{S}_4$ ¹⁶ and $\text{Li}_{10}\text{SnP}_2\text{S}_4$ ²⁶ are solid solutions of Li_4GeS_4 and Li_4SnS_4 with Li_3PS_4 in a molar ratio of 1:2. In general, these are group IV sulfides with group V sulfides. An intuitive question is whether Li_4SnS_4 and Li_3AsS_4 can form an ordered solid solution with a molar ratio of 1:2. To test this possibility, a composition with a 1:2 ratio of Sn to As was synthesized at temperatures of 400, 450 and 500°C. Powder XRD showed that such a composition does not form a homogeneous solid solution. Crystalline phases of Li_4SnS_4 and Li_3AsS_4 are clearly identified as components of the resulting mixture (Fig. S2 in the supporting information). The 1:2 ratio sample showed a relatively low ionic conductivity of 6.39×10^{-5} S/cm at room temperature. A simple mixture of Li_4SnS_4 and Li_3AsS_4 did not boost the conductivity. Therefore, a homogeneous solid solution is required for a good conduction phase.

Excellent air stability has been demonstrated

An important goal of this research is to achieve air stability of

sulfide-based solid electrolytes. According to the HSAB theory, the instability of the known Li P sulfides and Li Ge sulfides stems

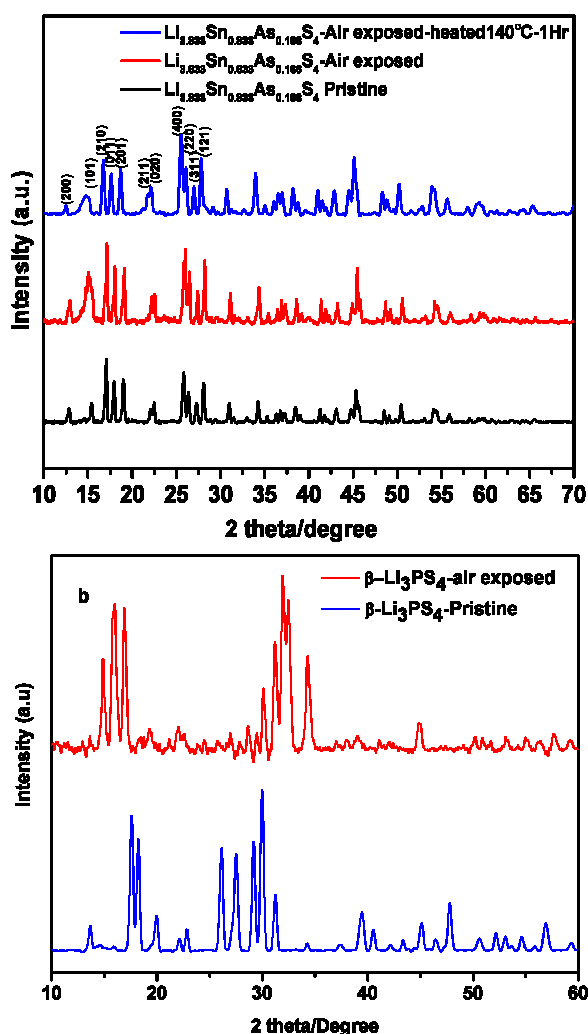


Fig. 3 Comparative structural evaluation upon air exposure. XRD patterns of (a) $\text{Li}_{3.833}\text{Sn}_{0.833}\text{As}_{0.166}\text{S}_4$ and (b) $\beta\text{-Li}_3\text{PS}_4$ before and after air exposure.

from the strong oxophilicity of the P and Ge atoms. The soft bases of Sn^{4+} and As^{5+} are expected to bind strongly with the soft base of S^{2-} . Therefore, these new solid electrolytes should be stable in air. To test the air stability, a representative sample of $\text{Li}_{3.833}\text{Sn}_{0.833}\text{As}_{0.166}\text{S}_4$ was shaken in ambient air for over 48 h. For comparison purposes, a sample of $\beta\text{-Li}_3\text{PS}_4$ was synthesized and shaken in ambient air at identical conditions.⁹ Figure 3a shows XRD spectra of pristine $\text{Li}_{3.833}\text{Sn}_{0.833}\text{As}_{0.166}\text{S}_4$ and after it had been exposed to laboratory ambience (64°F and 80% humidity) for 48 hours. The XRD peak intensity broadening at 16° after air exposure could be due to some absorbed moisture in the sample. In order to address this issue, the air exposed sample was heated at 140°C for 1 hour to remove any residual moisture content in the solid electrolyte. As expected, the peak intensity decreased significantly after the heat treatment and all the other peaks remained the same as the pristine sample. This fact indicates that the electrolyte is air stable because even with the small amount of absorbed moisture content, the sample showed very high ionic

conductivity. This is a clear piece of evidence to prove that the air exposure does not affect the intrinsic property of the solid electrolyte. The XRD patterns (Fig. 3b) of the control sample of $\beta\text{-Li}_3\text{PS}_4$ before and after air exposure are completely different.

The air exposure destroyed the crystal structure of $\beta\text{-Li}_3\text{PS}_4$.

The ionic conductivity of the pristine and air-exposed samples was measured by ac impedance. Figure 4 presents the temperature dependences of the conductivity of $\text{Li}_{3.833}\text{Sn}_{0.833}\text{As}_{0.166}\text{S}_4$ and $\beta\text{-Li}_3\text{PS}_4$ before and after exposure to air. The room-temperature ionic conductivities of $\text{Li}_{3.833}\text{Sn}_{0.833}\text{As}_{0.166}\text{S}_4$ before and after air exposure were $1.39 \times 10^{-3} \text{ Scm}^{-1}$ and $9.95 \times 10^{-4} \text{ Scm}^{-1}$, respectively. There is only a very minor change in conductivity, which may be due to a very

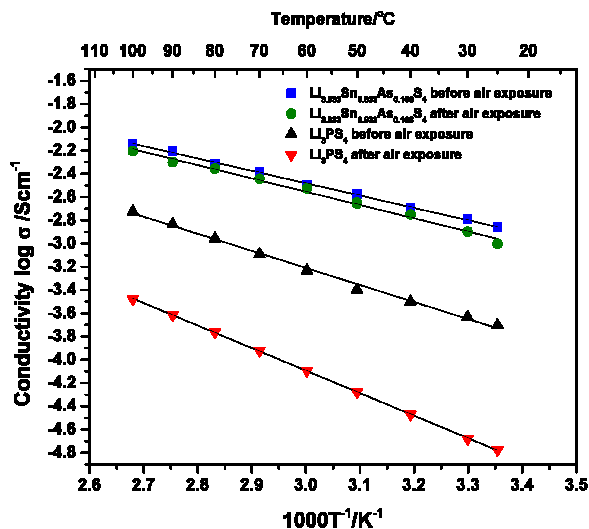


Fig. 4 Comparative Arrhenius plots for $\text{Li}_{3.833}\text{Sn}_{0.833}\text{As}_{0.166}\text{S}_4$ and $\beta\text{-Li}_3\text{PS}_4$ before and after air exposure.

small amount of moisture uptake or to variance in sample preparation. In stark contrast to the stable $\text{Li}_{3.833}\text{Sn}_{0.833}\text{As}_{0.166}\text{S}_4$ phase, the $\beta\text{-Li}_3\text{PS}_4$ showed more than an order of magnitude drop in ionic conductivity after air exposure.

Surface modification addresses chemical compatibility with

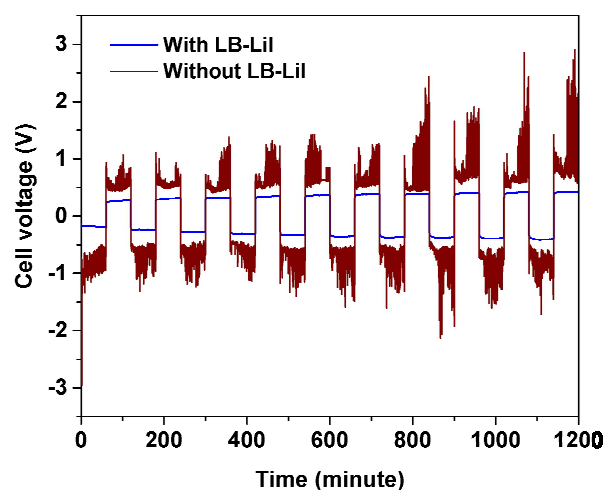


Fig. 5 Symmetric cell test before (red line) and after (black line) $3\text{LiBH}_4\text{LiI}$ coating, a current density of 0.1 mA cm^{-2} was applied to the cells.

metallic lithium

The most prominent advantage of a battery with a solid electrolyte is that it can employ a Li metal without the deleterious dendritic Li deposition typically seen in Li cells employing organic liquid electrolytes. Although some recently discovered sulfide-based solid electrolytes have sufficient ionic conductivity comparable to that of liquid electrolytes, the Ge and Sn atoms that impart the high Li-ion conductivity cause the incompatibility of these new materials with metallic Li. This work does not demonstrate an exception to that incompatibility with metallic Li. Since the electrolyte is in a solid form, it is possible to modify or passivate the surface of the electrolyte to achieve good compatibility with metallic Li. In this research, we demonstrate the concept of passivating the solid electrolyte by using a surface coating. The approach was to chemically passivate the surface of the solid electrolyte with a Li-compatible composite of $3\text{LiBH}_4\cdot\text{LiI}$ in THF solvent.¹⁹ A pellet of $\text{Li}_{3.833}\text{Sn}_{0.833}\text{As}_{0.166}\text{S}_4$ was dip-coated by a 5 wt. % $3\text{LiBH}_4\cdot\text{LiI}$ solution in THF. The THF was removed by heating the coated pellet to 170°C. Shown in Fig. 5 is a comparison of the symmetric cell cycling data before and after coating. The pristine pellet is not compatible with metallic Li electrodes. The cell voltage is spiky as a result of the interfacial reaction between the solid electrolyte and the newly deposited metallic Li. A smooth cell voltage was achieved after the $3\text{LiBH}_4\cdot\text{LiI}$ coating was applied. The coating material, $3\text{LiBH}_4\cdot\text{LiI}$, is a good ionic conductor that is compatible with metallic Li. The compatibility of the coated electrolyte with metallic lithium was further proved by the cyclic voltammetry (CV) measurement of $\text{Li}/\text{Li}_{3.833}\text{Sn}_{0.833}\text{As}_{0.166}\text{S}_4/\text{Pt}$ cell (Fig. S3). Li was the working and pseudo reference electrode and Pt was the counter electrode. The potential was scanned from -0.5 to 5.0 V vs. Li/Li^+ at a scan rate of 1mVs^{-1} . The cathodic current occurred right at 0V. This fact indicates that no side reaction happened during the lithium deposition. A sharp anodic peak was observed between 0 and 0.3V referring to lithium dissolution. A small peak was observed at 0.53 V, which is attributed to the dealloying of Li-Pt alloy formed at the electrochemical cycling. No additional peak was observed in the entire 5V electrochemical window. This proof-of-principle experiment opens an avenue for solving the compatibility problem of high-conduction Li-ion conductors.

Conclusions

Solid electrolytes with fast Li-ion conduction are a key requisite for enabling high-energy and safer all-solid-state Li batteries. Achieving high ionic conductivity, along with impressive chemical stability that facilitates battery processing, remains a grand challenge for the development of solid electrolytes. A new Li-ion conductor, $\text{Li}_{3.833}\text{Sn}_{0.833}\text{As}_{0.166}\text{S}_4$, was synthesized that showed a promising high Li ionic conductivity of $1.39\times 10^{-3}\text{Scm}^{-1}$ at room temperature and superior chemical stability when processed under air and/or moisture conditions. Various compositions of $\text{Li}_{4-x}\text{Sn}_{1-x}\text{As}_x\text{S}_4$ (where $x=0$ to 0.250) were systematically investigated through solid state synthesis. The results obtained were compared with the parent compound, Li_4SnS_4 . The ionic conductivity reached a maximum at a substitution level of 16.6% of Sn atoms replaced by As atoms.

Air stability was achieved based on the HSAB theory. Soft acids of As^{5+} and Sn^{4+} are intended to form a compound stable against hydrolysis and oxidation. Although chemical compatibility with metallic Li was compromised by the Sn and As atoms, surface modification of the solid electrolyte was demonstrated as a viable approach to retarding the interfacial reactions and therefore imparting excellent cyclability with metallic Li.

The toxicity and environmental impact of these new compounds are uncertain. Given the poisonous nature of As containing oxides, there could be a concern of toxicity regarding these sulfides. However, it is worth noting that many sulfur compounds of arsenic are known as occurring in nature, such as As_4S_3 in its α - and β -dimorphites.²⁷ Many others are produced industrially in bulk. Due to the insolubility of arsenic sulfides in water and acids, they are not dissolved in gastric juice and therefore they are not poisonous.²⁷ It will be an appropriate future topic to evaluate the toxicity and environmental impact of these compounds for their broad use in batteries.

Solid electrolytes and all-solid-state batteries are emerging research areas that are full of opportunities to address the increasing challenges of energy technologies. The application of HSAB theory in the design and the passivation of solid electrolytes will have a far-reaching impact on the development of high-energy batteries that are intrinsically safe.

Acknowledgment

This work was sponsored by the Division of Materials Sciences and Engineering, Office of Basic Energy Sciences US Department of Energy (DOE). The potential use of these electrolytes in lithium sulfur batteries was supported by U.S. Department of Energy (DOE)/Energy Efficiency and Renewable Energy (EERE) through Office of Vehicle Technologies. The synthesis and characterization of materials were conducted at the Center for Nanophase Materials Sciences, which is sponsored at Oak Ridge National Laboratory by the Scientific User Facilities Division, US DOE.

Notes and references

- (1) Center for Nanophase Materials Sciences; e-mail: liangcn@ornl.gov
 (2) Materials Science and Technology Division, Oak Ridge National Laboratory, Oak Ridge, TN 37831-6493, USA

† Electronic Supplementary Information (ESI) available: [details of any supplementary information available should be included here]. See DOI: 10.1039/b000000x/

References

- X. L. Ji and L. F. Nazar, *Journal of Materials Chemistry*, 2010, **20**, 9821-9826.
- C. D. Liang, N. J. Dudney and J. Y. Howe, *Chemistry of Materials*, 2009, **21**, 4724-4730.
- Z. Lin, Z. C. Liu, N. J. Dudney and C. D. Liang, *ACS Nano*, 2013, **7**, 2829-2833.
- Z. Lin, Z. C. Liu, W. J. Fu, N. J. Dudney and C. D. Liang, *Angew. Chem. Int. Ed.*, 2013, **52**, 7460-7463.
- J. W. Fergus, *J. Power Sources*, 2010, **195**, 4554-4569.
- P. Knauth, *Solid State Ionics*, 2009, **180**, 911-916.

7. S. Kondo, K. Takada and Y. Yamamura, *Solid State Ionics*, 1992, **53**, 1183-1186.
8. K. Takada, N. Aotani and S. Kondo, *J. Power Sources*, 1993, **43**, 135-141.
9. Z. Liu, W. Fu, E. A. Payzant, X. Yu, Z. Wu, N. J. Dudney, J. Kiggans, K. Hong, A. J. Rondinone and C. Liang, *J Am Chem Soc.*, 2013, **135**, 975-978.
10. Y. Inaguma, L. Q. Chen, M. Itoh, T. Nakamura, T. Uchida, H. Ikuta and M. Wakihara, *Solid State Communications*, 1993, **86**, 689-693.
11. A. Hayashi, S. Hama, H. Morimoto, M. Tatsumisago and T. Minami, *Journal of the American Ceramic Society*, 2001, **84**, 477-479.
12. K. Aso, A. Sakuda, A. Hayashi and M. Tatsumisago, *ACS Applied Materials Interfaces*, 2013, **5**, 686-690.
13. F. Mizuno, A. Hayashi, K. Tadanaga and M. Tatsumisago, *Adv. Mater.*, 2005, **17**, 918-921.
14. R. Kanno and M. Maruyama, *J. Electrochem. Soc.*, 2001, **148**, A742-A746.
15. R. Kanno, M. Murayama and K. Sakamoto, *New lithium solid electrolytes, thio-lisicon: Materials design concept and application to solid state battery*, **2002**.
16. N. Kamaya, K. Homma, Y. Yamakawa, M. Hirayama, R. Kanno, M. Yonemura, T. Kamiyama, Y. Kato, S. Hama, K. Kawamoto and A. Mitsui, *Nat. Mater.*, 2011, **10**, 682-686.
17. K. Takada, *Acta Materialia*, 2013, **61**, 759-770.
18. T. Kaib, S. Haddadpour, M. Kapitein, P. Bron, C. Schroder, H. Eckert, B. Roling and S. Dehnen, *Chemistry of Materials*, 2012, **24**, 2211-2219.
19. H. Maekawa, M. Matsuo, H. Takamura, M. Ando, Y. Noda, T. Karahashi and S. I. Orimo, *Journal of the American Chemical Society*, 2009, **131**, 894-+.
20. L. O. Valoen and J. N. Reimers, *J. Electrochem. Soc.*, 2005, **152**, A882-A891.
21. T. Fromling, M. Kunze, M. Schonhoff, J. Sundermeyer and B. Roling, *Journal of Physical Chemistry B*, 2008, **112**, 12985-12990.
22. M. Watanabe, S. Nagano, K. Sanui and N. Ogata, *Solid State Ionics*, 1988, **28**, 911-917.
23. M. Tachez, J. P. Malugani, R. Mercier and G. Robert, *Solid State Ionics*, 1984, **14**, 181-185.
24. E. Rangasamy, J. Wolfenstine and J. Sakamoto, *Solid State Ionics*, 2012, **206**, 28-32.
25. R. D. Shannon, *Acta Crystallogr. Sect. A*, 1976, **32**, 751-767.
26. P. Bron, S. Johansson, K. Zick, J. Schmedt auf der Günne, S. S. Dehnen and B. Roling, *Journal of the American Chemical Society*, 2013.
27. N. Wiberg, A. F. Holleman and E. Wiberg, *Holleman-Wiberg's Inorganic Chemistry*, Academic Press; 1 edition (November 5, 2001).

Supporting Information

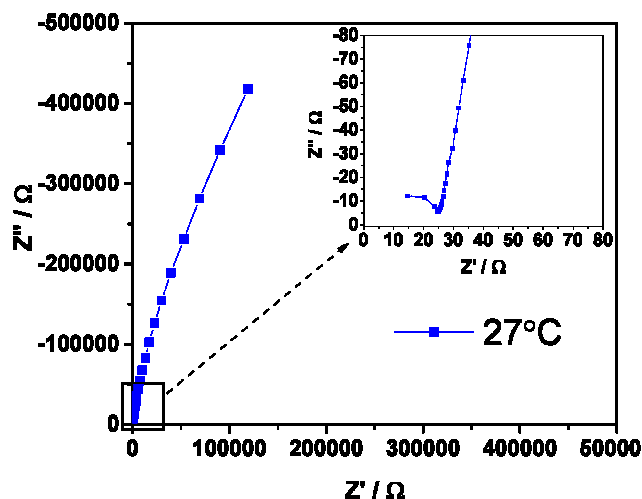


Fig. S1. Impedance spectrum of $\text{Li}_{3.833}\text{Sn}_{0.833}\text{As}_{0.166}\text{S}_4$ measured at room temperature. The total conductivity is determined by using the intercept between the semi-arc and straight line as the total resistance.

Powder XRD pattern of Li_4SnS_4 and Li_3AsS_4 with a molar ratio of 1:2 synthesized at identical conditions of the $\text{Li}_{3.833}\text{Sn}_{0.833}\text{As}_{0.166}\text{S}_4$ phase.

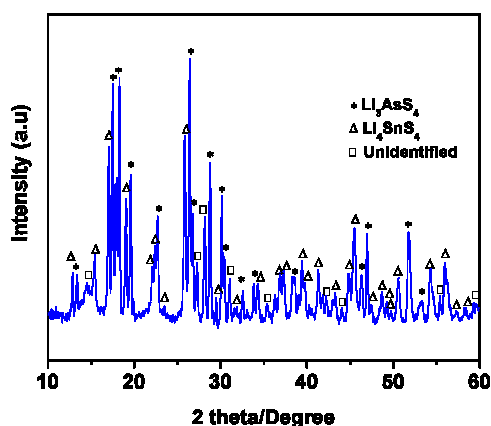


Fig. S2 Powder XRD pattern of As-substituted Li_4SnS_4 with a nominal composition of $\text{Li}_{10}\text{SnAs}_2\text{S}_{12}$ synthesized at identical conditions of $\text{Li}_{3.833}\text{Sn}_{0.833}\text{As}_{0.166}\text{S}_4$

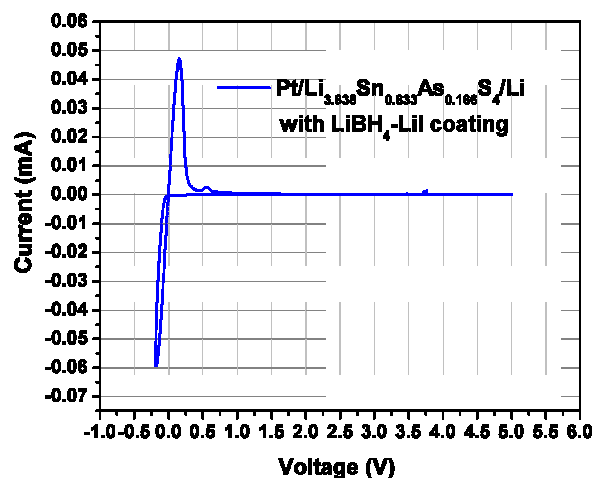


Fig. S3. Cyclic voltammogram of a $\text{Pt}/\text{Li}_{3.838}\text{Sn}_{0.838}\text{As}_{0.166}\text{S}_4/\text{Li}$ cell with $\text{LiBH}_4\text{-LiI}$ passivation layer at 1 mVs^{-1} showing plating and stripping of Li between -0.5 and 5.0 V .

Table S1 Comparison of activation energy of various solid electrolytes

Solid Electrolytes	Activation Energy E_a (eV)	References
$\text{Li}_{10}\text{GeP}_2\text{S}_{12}$ (LGPS)	0.24	[9]
Nanoporous $\beta\text{-Li}_3\text{PS}_4$ ($\beta\text{-LPS}$)	0.35	[16]
Bulk $\beta\text{-Li}_3\text{PS}_4$	0.47	[23]
Hot pressed cubic $\text{Li}_7\text{La}_3\text{Zr}_2\text{O}_{12}$ (LLZO)	0.26	[24]
$\text{Li}_{3.838}\text{Sn}_{0.833}\text{As}_{0.166}\text{S}_4$	0.21	Our new electrolyte